




Interactions-disorder duality and critical phenomena in nodal semimetals, dilute gases, and other systems

Shijun Sun  and Sergey Syzranov 

Physics Department, University of California, Santa Cruz, California 95064, USA

 (Received 19 May 2021; revised 25 July 2023; accepted 30 October 2023; published 15 November 2023)

We investigate classes of interacting systems that allow for a mapping to disordered noninteracting systems. As we show, such a mapping is possible for interacting systems with a suppressed density of states at the chemical potential, leading to suppressed screening, and systems near BCS-type instabilities. The mapping can also be applied qualitatively to other classes of systems that are approximately dual to each other. The established duality suggests a new approach to analytical and numerical studies of many-body and disorder-driven phenomena in a variety of systems and allows to predict, e.g., new phase transitions dual to the previously known ones. Using the established duality, we predict new disorder-driven transitions in nodal-line semimetals and systems with long-range hopping dual to, respectively, the BCS and BEC-vacuum transitions in interacting systems and new interaction-driven transitions dual to previously known non-Anderson disorder-driven transitions. The established principle can also be used to classify and describe phase transitions in dissipative systems described by non-Hermitian Hamiltonians.

DOI: [10.1103/PhysRevB.108.195132](https://doi.org/10.1103/PhysRevB.108.195132)

I. INTRODUCTION

Describing many-body interacting systems is one of the greatest challenges in physics. Often, existing analytical approaches are insufficient to accurately describe many-body effects, such as high-temperature superconductivity, interaction-driven metal-insulator transition, and magnetic instabilities.

Simulating such systems numerically is also a formidable task, especially in the case of fermionic (quasi-)particles, which display the notorious sign problem [1–3] leading to a rapid growth of the computation time with the number of particles. By contrast, single-particle problems, even in the presence of quenched disorder, may be comparatively easily simulated, e.g., by diagonalizing the Hamiltonian of the system.

Disorder-averaged observables in single-particle models, however, are described by interacting field theories in the supersymmetric [4], Keldysh [5], or replica [6] representations. Such theories have the same form as the field theories of interacting disorder-free systems but have additional structures in, respectively, boson-fermion, Keldysh, or replica subspaces. It is natural to expect, therefore, that a certain class of many-body systems may be mapped to single-particle disordered models.

Such a duality would allow one to predict new many-body (disorder-driven) phenomena, e.g., phase transitions, dual to previously known disorder-driven (many-body) effects. It would also allow for numerical simulations of many-body effects in the systems that have single-particle duals using the methods of disordered systems. The purpose of this paper is to explore such a duality between interacting and disordered noninteracting systems, identify classes of systems that allow for the duality, and reveal novel critical phenomena resulting from the duality.

We demonstrate that such a duality indeed exists for broad classes of interacting and disordered systems and interaction- and disorder-driven phenomena. Such phenomena include, but are not limited to, ultraviolet (UV) effects [7,8], i.e., transport effects and phase transitions that come from quasiparticle scattering through states far from the chemical potential (in a momentum band exceeding the inverse mean free path ℓ^{-1}). Such phenomena include (I) effects in nodal semimetals and systems in sufficiently high dimensions (unconventional quantum corrections to transport [9], non-Anderson disorder-driven transitions [7], unconventional superconductive instabilities [10,11], etc.) and (II) BCS-type interaction-driven instabilities with a single interaction channel. The duality transformation that we derive can also be applied to other systems to reveal new phenomena that are not exactly dual but similar to the previously known ones.

The duality transformation we develop in this paper maps a d -dimensional interacting disorder-free system to a $d + 1$ -dimensional noninteracting system with quenched disorder and an additional (pseudospin) degree of freedom equivalent to a spin-1/2. The mapping is accurate if the screening of the interactions can be neglected, as is the case for systems I and II mentioned above.

The existence of such a duality mapping for nodal semimetals is consistent with the well-known [2] absence of the numerical sign problem in systems with particle-hole symmetry. Indeed, nodal semimetals with symmetric valence and conduction bands and chemical potentials close to the band-touching point (see Fig. 1) have (approximate) particle-hole symmetry.

The mapping we derive suggests, in particular, that interacting electronic systems with a vanishing DoS at the Fermi level exhibit interaction-driven phase transitions in the

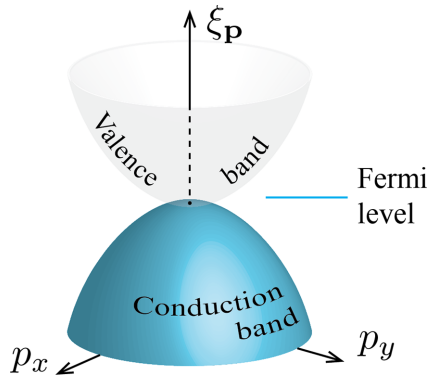


FIG. 1. The band structure of a nodal semimetal. For the power-law dispersion $\propto p^\alpha$, the density of states $\rho(\varepsilon) \propto |\varepsilon|^{\frac{d}{\alpha}-1}$ is suppressed in high dimensions $d > \alpha$, which leads to a suppressed screening of the interactions.

universality classes of the non-Anderson disorder-driven phase transitions [7,12–17] that have been established, at the perturbative level, to take place in noninteracting semimetals in high spacial dimensions, exemplified by three-dimensional (3D) Weyl semimetals. Using the duality demonstrated in this paper, we find a new non-Anderson disorder-driven phase transition dual to the previously known “vacuum-BEC” transition [18–20]. Furthermore, we predict new disorder-driven transitions dual to the interaction-driven BCS-type transitions (e.g., superconductive and excitonic instabilities). Such transitions lead, for example, to the critical scaling of the density of states in disordered nodal-line semimetals [8]. The duality can be extended further to the case of non-Hermitian Hamiltonians and phase transitions.

The paper is organized as follows. We summarize the duality mapping and classes of dual systems in Sec. II. In Sec. III A, we provide a heuristic argument for the mapping, followed by a rigorous derivation of the duality to all orders in perturbation theory in Sec. III B. Section IV is devoted to three examples of dual phenomena between disordered and interacting systems, showing how, e.g., new phase transitions can be predicted using the established duality. We conclude in Sec. V.

II. SUMMARY OF THE MAPPING

We consider d -dimensional interacting systems described by Hamiltonians of the form

$$\hat{\mathcal{H}} = \int \hat{\Psi}^\dagger(\mathbf{r}) \xi_{\mathbf{p}} \hat{\Psi}(\mathbf{r}) d^d \mathbf{r} - \frac{1}{2} \int \hat{\Psi}^\dagger(\mathbf{r}) \hat{\Psi}^\dagger(\mathbf{r}') U(\mathbf{r} - \mathbf{r}') \hat{\Psi}(\mathbf{r}') \hat{\Psi}(\mathbf{r}) d^d \mathbf{r} d^d \mathbf{r}', \quad (1)$$

where $\hat{\Psi}^{(\dagger)}$ are the particle operators, $\xi_{\mathbf{p}}$ is the single-particle dispersion, $\hat{\mathbf{p}} = -i\partial_{\mathbf{r}}$ is the momentum operator (hereinafter $\hbar = 1$), and the potential $U(\mathbf{r} - \mathbf{r}')$ describes the interactions. The particles may be bosonic or fermionic. While we consider, for simplicity, spinless particles, the mapping described in this paper can be generalized to account for an arbitrary spin structure of the dispersion and the interaction.

We assume that the screening is either suppressed or has no qualitative effects on the observables and phenomena of interest, i.e., does not change the universality class of a phase transition. This is often the case for phenomena dominated by the *ultraviolet* energy and momentum scales.

For example, in nodal semimetals and gases with the power-law dispersion $\xi_{\mathbf{p}} \propto p^\alpha$ (possibly with an additional structure in the spin/valley space) in high dimensions $d > \alpha$, the screening will be suppressed due to the suppressed density of states, $\rho(\varepsilon) \propto |\varepsilon|^{\frac{d}{\alpha}-1}$, at the node or a band touching point ($k = 0$). $\alpha = 1$ corresponds to graphene in the dimension $d = 2$ and to 3D Weyl/Dirac semimetals in the dimension $d = 3$. The case $\alpha = 2$ describes semiconductors and parabolic semimetals. Dispersions with a continuously tunable parameter α may be realized in systems of trapped ultracold particles [21–24] and superconductive films [25]. Furthermore, d -dimensional systems with long-range hopping $\propto 1/r^{d-\alpha}$, also realized with trapped ultracold particles, can be mapped to systems with the power-law dispersion $\xi_{\mathbf{p}} \propto p^\alpha$ [26].

For some phenomena, such as BCS-type instabilities (superconductive or exciton-condensation instabilities) or leading-order correlators of electron densities, screening is not important even in the presence of a large Fermi surface.

For the case of *attractive interactions*, on which we focus in most of this paper, the behavior of observables in an interacting disorder-free d -dimensional system described by the Hamiltonian (1) can be mapped to the behavior of disorder-averaged observables in a $d + 1$ -dimensional noninteracting semimetal with the Hamiltonian

$$\hat{h} = \hat{\sigma}_z \xi_{\mathbf{p}} + \hat{\sigma}_y p_{d+1} + \hat{\sigma}_z u(\boldsymbol{\rho}), \quad (2)$$

where $\hat{\sigma}_x$, $\hat{\sigma}_y$, and $\hat{\sigma}_z$ are the Pauli matrices corresponding to a degree of freedom equivalent to a spin-1/2, hereinafter referred to as *pseudospin*; \mathbf{p} is the momentum of the particle along the first d dimensions; p_{d+1} is the component of momentum along the $d + 1$ -st dimension; $u(\boldsymbol{\rho})$ is a random potential in the $d + 1$ -dimensional space whose correlator $-D(\mathbf{r}, \tau; \mathbf{r}', \tau')$ is given by the propagator of the interactions in Eq. (1). For short-ranged interactions, the strength of both the interactions and the random potential are described by one coupling constant

$$g = \int U(\mathbf{r} - \mathbf{r}') d^d \mathbf{r}' = \int \langle u(\boldsymbol{\rho}) u(\boldsymbol{\rho}') \rangle_{\text{dis}} d^{d+1} \boldsymbol{\rho}'. \quad (3)$$

Along the $d + 1$ -st dimension, the size of the system described by the Hamiltonian (2) is given by $\ell_{d+1} = 1/T$, where T is the temperature of the interacting system with the Hamiltonian (1) and (anti-)periodic conditions are imposed for (fermionic) bosonic particles. Some of the dual quantities in the disordered and interacting models are listed in Table I.

The mapping can be similarly carried out for *repulsive interactions*, with the Hamiltonian (2) replaced by

$$\hat{h}_{\text{repulsive}} = \hat{\sigma}_z \xi_{\mathbf{p}} + \hat{\sigma}_y p_{d+1} + \hat{\sigma}_y u(\boldsymbol{\rho}). \quad (4)$$

Each observable in the interacting model (1) corresponds to a disorder-averaged quantity in the disordered noninteracting model (2). For example, the average density $\hat{n}(\mathbf{r}) = \hat{\Psi}^\dagger(\mathbf{r}) \hat{\Psi}(\mathbf{r})$ of the interacting particles matches, as a function of the disorder/interaction strength (e.g., coupling g), the

TABLE I. Correspondence between quantities in the interacting disorder-free and noninteracting disordered systems.

	Interacting model	Disordered model
Coordinates	(τ, \mathbf{r})	$(\mathbf{r}_{d+1}, \mathbf{r})$
Temperature/size	T	$1/\ell_{d+1}$
Interaction potential/ disorder correlation	$U(\mathbf{r} - \mathbf{r}')$	$\langle u(\mathbf{r}_{d+1}, \mathbf{r})u(\mathbf{r}_{d+1}, \mathbf{r}') \rangle_{\text{dis}}$
Observables	\hat{n} (density)	ρ_s , Eq. (5)

disorder-averaged quantity,

$$\rho_s(\boldsymbol{\rho}) = \frac{1}{4} \text{Tr}[\hat{\sigma}_z \hat{G}^R(\boldsymbol{\rho}, \boldsymbol{\rho}, 0) + \hat{\sigma}_z \hat{G}^A(\boldsymbol{\rho}, \boldsymbol{\rho}, 0)], \quad (5)$$

in the dual disordered noninteracting system, where Tr is taken over the pseudospin degree of freedom and $\hat{G}^R(\boldsymbol{\rho}, \boldsymbol{\rho}, E)$ and $\hat{G}^A(\boldsymbol{\rho}, \boldsymbol{\rho}, E)$ are the matrices of the retarded and advanced Green's functions of the particles in the pseudospin space. Similar correspondence can be established for other observables, such as currents and spin densities.

Types of dual systems

There are multiple types of disordered systems described by the Hamiltonian (2) [Eq. (4)] and dual interacting systems. They include several broad classes: (I) If $\xi_{\mathbf{p}}$ vanishes at a point ($\mathbf{p} = 0$), then the duality provides a mapping between an interacting nodal-point semimetal and a disordered anisotropic nodal semimetal in a higher dimension; (II) if $\xi_{\mathbf{p}}$ vanishes along a line in momentum space, then a generic 2D interacting metal is mapped to a 3D disordered nodal-line semimetal; (III) at very high temperatures T in the interacting system, the motion of the dual disordered system is strongly constrained (quantized) along the $d + 1$ -st dimension and is reduced to the d -dimensional motion of a particle in a random potential with the generic Hamiltonian $\hat{h}_{\text{eff}} = \xi_{\mathbf{p}} + u(\boldsymbol{\rho})$.

For all of these types of systems, the derived mapping reveals new critical phenomena dual to previously known ones, as detailed below. For systems in groups I and II, the duality is accurate under the conditions discussed in the introduction. In Sec. IV, we review some of the phenomena revealed for such systems by the duality mapping derived in this paper.

For systems in group III, the assumption about the negligibility of interactions is, in general, not fulfilled. Nevertheless, the mapping allows us to predict a high-temperature interaction-driven transition in a system with the power-law dispersion $\xi_{\mathbf{p}} \propto p^\alpha$ associated by the duality mapping with the non-Anderson disorder-driven transitions [7] for particles with the same dispersion in the same dimension. We will provide a detailed description of such interaction-driven transitions elsewhere [27].

III. DERIVATION OF THE DUALITY

A. Heuristic argument

The mapping can be understood intuitively from the following heuristic argument. The partition function of a d -dimensional system with the attractive-interaction term

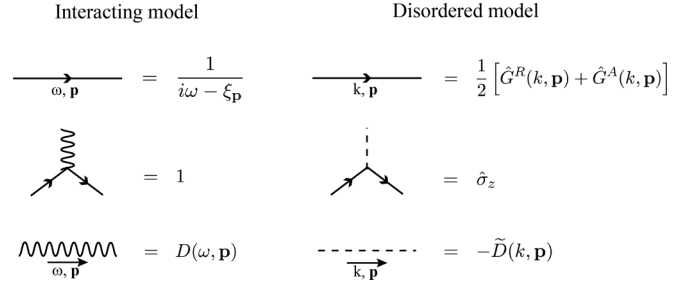


FIG. 2. Elements of the diagrammatic technique for the interacting disorder-free (left) and noninteracting disordered (right) models in momentum space that illustrate perturbative equivalence between the two classes of systems.

decoupled by the Hubbard-Stratonovich field $\phi(\mathbf{r}, \tau)$

$$Z = \int \mathcal{D}\bar{\psi} \mathcal{D}\psi \mathcal{D}\phi \exp \left[- \int \bar{\psi} (\partial_\tau + \xi_{\mathbf{p}} + \phi) \psi d^d \mathbf{r} d\tau - \frac{1}{2} \int \phi(\tau, \mathbf{r}) U^{-1}(\mathbf{r}, \mathbf{r}') \phi(\tau, \mathbf{r}') d\tau d^d \mathbf{r} d^d \mathbf{r}' \right] \quad (6)$$

resembles the partition function of a disordered $d + 1$ -dimensional system, where the Matsubara time τ is considered as an extra coordinate, with a non-Hermitian Hamiltonian $\tilde{h} = \partial_\tau + \xi_{\mathbf{p}} + \phi$ and ϕ playing the role of the disorder potential.

The procedure of “Hermitization” [28–33] can be applied then to associate the non-Hermitian operator $\tilde{h} = \partial_\tau + \xi_{\mathbf{p}} + \phi$ with its “Hermitized” version $\tilde{h}_{\text{herm}} = \hat{\sigma}_x p_\tau + \hat{\sigma}_y \xi_{\mathbf{k}} + \hat{\sigma}_y \phi$ in the doubled Hilbert space, where $p_\tau = -i\partial_\tau$. The “Hermitized” Hamiltonian matches, up to a rotation of the pseudospin basis, the Hamiltonian (2). The properties of this Hamiltonian are similar to those of \tilde{h} and allow for obtaining related observables.

Another distinction of the action (6) from that of a disordered system is that it uses Grassmann (real) fields $\bar{\psi}$ and ψ for fermionic (bosonic) particles not including the fermion-boson, replica or Keldysh subspaces inherently present in field theories of disordered systems. As a result, it allows, in general, for “loop” contributions to observables that account for, e.g., the screening of the interactions and that are absent in disordered field theories [4,34,35]. Under the assumptions we make in this paper, however, such contributions are negligible.

B. Perturbative derivation

The summarized duality can be rigorously verified to all orders of the perturbation theory under the made approximations, with the corresponding elements of the diagrammatic technique shown in Fig. 2.

For example, perturbative contributions to the average density of particles \hat{n} in the interacting system described by Hamiltonian (1) are shown in Figs. 3(a)–3(c). The diagrams in Fig. 3(a) include, apart from the interaction propagators (wiggly lines), only one loop of particle propagators (solid lines). Contributions with additional loops of propagators, exemplified by Figs. 3(b) and 3(c), can be neglected. Some of those neglected contributions [Fig. 3(b)] describe the screening of the interactions. The others contain a loop connected

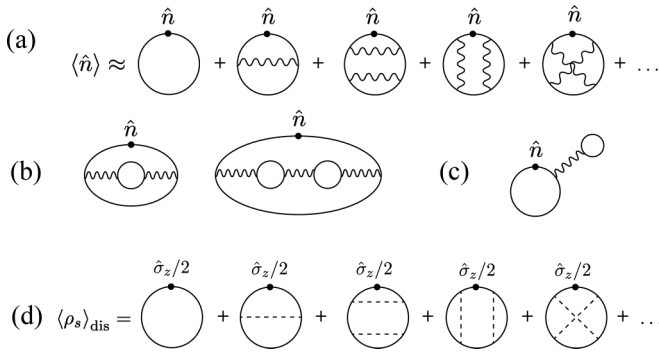


FIG. 3. Diagrams for observables in dual interacting disorder-free and noninteracting disordered systems. (a) Contributions to the concentration of interacting particles. [(b) and (c)] Examples of neglected contributions; diagrams (b) are neglected due to the screening suppression; (c) is the Hartree contribution. (d) Corresponding contributions to the disorder averaged quantity ρ_s , given by Eq. (5) in the disordered noninteracting system.

to the rest of the diagram by a single interaction propagator [Hartree-type contributions, shown in Fig. 3(c)] which may be absorbed in the definition of the chemical potential and has no qualitative effects.

Each of the remaining diagrams for the interaction system [Fig. 3(a)] corresponds to a diagram for the dual disordered system [Fig. 3(c)]. A diagram of the interaction system is mapped to a diagram in the dual disordered system by replacing the interaction propagators with the disordered lines (dashed lines). In what immediately follows, we demonstrate that the values of the respective diagrams in the interacting and disordered systems described by the Hamiltonians (1) and (2) (4) match. Indeed, for point interactions, the value of a diagram with N interaction propagators contributing to the density of particles in the interacting system is given by

$$\pm \frac{g^N T^{N+1}}{V^{N+1}} \sum_{\omega, \mathbf{p}} \frac{1}{(i\omega_1 - \xi_{\mathbf{p}_1})^2} \frac{1}{i\omega_2 - \xi_{\mathbf{p}_2}} \cdots \frac{1}{i\omega_{2N} - \xi_{\mathbf{p}_{2N}}}, \quad (7)$$

where “+” and “−” signs correspond to bosonic and fermionic particles, g is the coupling constant, T and V are the temperature and volume of the system, respectively; the sum is carried over any $N + 1$ independent frequencies and momenta with the rest of the frequencies and momenta determined from the energy and momentum conservation laws in the diagram. Each sum with respect to Matsubara frequencies ω in Eq. (7) can be replaced with two summations with respect to ω and $-\omega$, $\sum_{\omega} \dots = \frac{1}{2} \sum_{\omega} \dots + \frac{1}{2} \sum_{-\omega} \dots$, which gives

$$\pm \frac{g^N T^{N+1}}{2V^{N+1}} \sum_{\sigma=\pm 1} \sum_{\omega, \mathbf{p}} \frac{1}{(i\omega_1 \sigma - \xi_{\mathbf{p}_1})^2} \frac{1}{i\omega_2 \sigma - \xi_{\mathbf{p}_2}} \cdots \frac{1}{i\omega_{2N} \sigma - \xi_{\mathbf{p}_{2N}}}. \quad (8)$$

The value of the corresponding diagram in the dual disordered noninteracting system contributing to the dual disorder-averaged quantity ρ_s with N disordered lines is given

by

$$\pm \frac{g^N}{2V^{N+1} \ell_{d+1}^{N+1}} \sum_{\mathbf{p}, k} \text{Tr} \left[\frac{1}{ik_1 \hat{\sigma}_x - \xi_{\mathbf{p}_1} \mathbb{1}_{2 \times 2}} \frac{1}{ik_1 \hat{\sigma}_x - \xi_{\mathbf{p}_1} \mathbb{1}_{2 \times 2}} \cdots \frac{1}{ik_{2N} \hat{\sigma}_x - \xi_{\mathbf{p}_{2N}} \mathbb{1}_{2 \times 2}} \right], \quad (9)$$

as follows from the diagrammatic rules summarized in Fig. 2. Here the “+” and “−” signs correspond to periodic and antiperiodic boundary conditions along the $d + 1$ -st dimension, g is the coupling constant now describing the strength of short-range correlated random potential, the dual disordered system has a volume of $V \ell_{d+1}$, the trace $\text{Tr}[\dots]$ is taken over the pseudospin degrees of freedom, and $\mathbb{1}_{2 \times 2}$ is the 2×2 identity matrix in the pseudospin space.

The value (8) of the diagram for the interacting disorder-free system matches the value (9) of the respective diagram for the noninteracting disordered system. Indeed, since all the propagators in the square bracket in Eq. (9) commute with each other in the pseudospin space, one can replace the operator $\hat{\sigma}_x$ with its eigenvalues $\sigma_x = \pm 1$ in the denominators (the same for all propagators). Since according to the duality transformation (cf. Table I), the temperature T of the interacting system matches the inverse length ℓ_{d+1} and (fermionic) bosonic particles correspond to (anti-)periodic boundary conditions, expressions (9) and (8) match.

In Appendix A, we extend the arguments of this section to generic finite-range interactions and correlations of the random potential and provide explicit expressions for contributions to observables in dual interacting and disordered systems to first several orders of the perturbation theory.

IV. EXAMPLES

In this section, we provide several examples of dual phenomena in disordered and interacting systems mentioned in Sec. II.

A. Duality between a 2D metal and 3D nodal-line semimetal

The dispersion $\xi_{\mathbf{p}}$ is measured from the chemical potential and, in general, vanishes on a finite surface, $\xi_{\mathbf{p}} = 0$, in momentum space. For a 2D interacting metal, this surface is a line, and the dual disordered Hamiltonian (2) describes a 3D nodal-line semimetal, i.e., a semimetal with two bands touching along a line in momentum space [36].

Although the density of states is not suppressed for a 2D metal, the duality can be applied if the screening of the interactions has no qualitative effects, e.g., does not change the universality class of a phase transition, such as at the superconductive (BCS-type) instability. We predict, therefore, that a 3D nodal-line semimetal exhibits a disorder-driven transition dual to the BCS transition in a 2D semimetal. A microscopic derivation of such a transition is presented in a separate work [8].

B. Disorder-driven transition dual to the BCS-BEC transition

A broad class of interacting systems that satisfies the assumptions used to derive the duality corresponds to the dispersion $\xi_{\mathbf{p}}$ that vanishes at a point ($\mathbf{p} = 0$) in momentum

space, e.g., at the bottom of the dispersion in an interacting gas or near the band touching point in a nodal-point semimetal (for example, Dirac, Weyl or parabolic semimetal). For the power-law dispersion, $\xi_{\mathbf{p}} \propto p^\alpha$, a d -dimensional interacting system is mapped to an anisotropic disordered nodal-point semimetal with the dispersion $\xi_{\mathbf{p}}\hat{\sigma}_z + p_{d+1}\hat{\sigma}_y$.

Interacting nodal-point semimetals display a variety of instabilities at low temperatures (see, for example, Refs. [11,37–42]), such as superconductive, magnetic and charge-density-wave phase transitions. By contrast, noninteracting disordered systems are commonly believed to exhibit only one phase transition: the Anderson localization-delocalization transition. However, it has been demonstrated, at the perturbative level, that semimetals and semiconductors with the power-law dispersion $\propto p^\delta$ in high dimensions $\tilde{d} > 2\delta$ exhibit additional disorder-driven transitions (see Ref. [7] for a review) in non-Anderson universality classes [43]. These non-Anderson disorder-driven transitions may have diverse properties depending on the symmetries of the disorder and of the band structure, and, under some approximations [43], display a critical behavior of the density of states [16,17,44–57], in contrast with the Anderson transitions.

The duality allows us to predict a new non-Anderson disorder-driven transition, distinct from all the previously studied transitions, in semimetals with the Hamiltonian (2) in which the dispersion $\xi_{\mathbf{p}}$ vanishes at small momenta. This transition is dual to the so-called vacuum-BEC transition [18] in systems of interacting bosons with attractive interactions [19,20,58].

For $\xi_{\mathbf{p}} \propto p^\alpha$ and short-range interactions (disorder), the instability for both interacting and disordered systems can be demonstrated by the renormalization-group (RG) analysis of the dimensionless coupling constant

$$\gamma = \frac{\zeta S_d}{2(2\pi)^d} g K^{d-\alpha}, \quad (10)$$

where S_d is the volume of a unit d -dimensional sphere; K is the ultraviolet momentum cutoff, e.g., the characteristic size of the band in momentum space; and ζ is a factor of order unity that depends on the spin and valley structure of the dispersion near the node or the band edge ($\zeta = 1$ for $\xi_{\mathbf{k}} = k^\alpha$). On integrating out the highest momentum modes of the particles in both systems (see Appendix B), the flow of the dimensionless coupling is given by the (exact) RG equation

$$\partial_l \gamma = (\alpha - d)\gamma + \gamma^2, \quad (11)$$

which signals a phase transition (in systems with attractive interactions, $g > 0$) in high dimensions $d > \alpha$ at the critical coupling $\gamma_c = d - \alpha$.

For interacting bosons, the corresponding transition occurs between a phase with effectively noninteracting particles (“vacuum”) and a phase of strongly coupled bosons that form Bose-Einstein condensate (BEC) in dimension d . The dual $d + 1$ -dimensional disorder-driven phase transition, which we predict here, occurs, respectively, between a phase with effectively vanishing disorder and a strongly disordered phase. This disorder-driven transition manifests itself in the critical behavior of observables, such as the density of states and transport coefficients in the system. In contrast with the

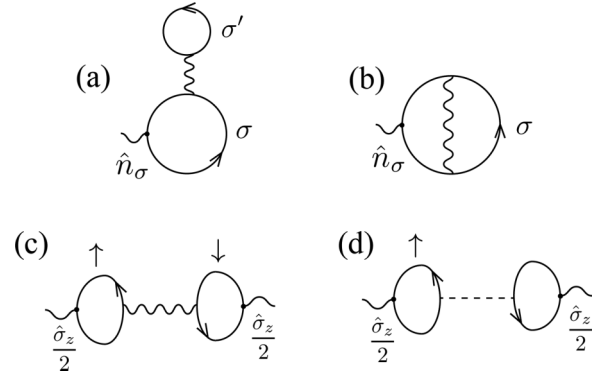


FIG. 4. Diagrams for correlations in the one-site Hubbard model and a disordered wire. [(a) and (b)] Modifications to the number n_σ of the particles with spin σ but do not affect the correlations between n_\uparrow and n_\downarrow mimicked by (c) to the first order in the interaction g . (d) Correlations in the dual noninteracting disordered system.

previously studied non-Anderson disorder-driven transitions [7] the instability predicted here is described exactly by the RG Eq. (11), which allows for an exact determination of the correlation-length critical exponent $\nu = 1/(d - \alpha)$.

C. Electronic correlations in a quantum dot and a 1D disordered wire

Above, we described classes of interacting and disordered systems that are associated to each other by the derived duality mapping. In what immediately follows, we demonstrate that the mapping can generically be applied to correlators of observables, e.g., electron densities, if they are considered to the leading order in interactions, in which they are not affected by screening and the Hartree contributions. To illustrate this, we consider a one-site Hubbard model (quantum dot) described by the Hamiltonian

$$\hat{\mathcal{H}}_{\text{dot}} = \xi \hat{n}_\uparrow + \xi \hat{n}_\downarrow - g \hat{n}_\uparrow \hat{n}_\downarrow, \quad (12)$$

where ξ is a constant and n_\uparrow and n_\downarrow are the numbers of the electrons in the “spin-up” and “spin-down” states. This quantum dot is dual to a system of a 1D particle in a random potential $u(x)$, with the Hamiltonian given by

$$\hat{h}_{\text{wire}} = \sum_{i=\uparrow,\downarrow} \hat{\Psi}_i(x) [\xi \hat{\sigma}_z - i \hat{\sigma}_y \partial_x + u(x) \hat{\sigma}_z] \hat{\Psi}_i(x). \quad (13)$$

In general, perturbative contributions with loops are not negligible for electrons in a quantum dot described by the Hamiltonian (12). For example, the Hartree contribution to the number of electrons n_σ with spin σ in Fig. 4(a) matches the value of Fig. 4(b). These contributions, however, do not affect, to the first order in the coupling g , the correlator

$$K = \langle \hat{n}_\uparrow \hat{n}_\downarrow \rangle - \langle \hat{n}_\uparrow \rangle \langle \hat{n}_\downarrow \rangle = \frac{g}{T} \left[\frac{e^{\xi/T}}{(1 + e^{\xi/T})^2} \right]^2 + \mathcal{O}(g^2) \quad (14)$$

of the numbers n_\uparrow and n_\downarrow of fermions with different spins computed in Appendix C. The value of the correlator (14)

matches, to the leading order in g , the correlator

$$K_{\text{dis}} = \langle \rho_{s\uparrow} \rho_{s\downarrow} \rangle_{\text{dis}} - \langle \rho_{s\uparrow} \rangle_{\text{dis}} \langle \rho_{s\downarrow} \rangle_{\text{dis}} \quad (15)$$

of the operators ρ_s given by Eq. (5). The value of the correlator (15) is computed independently for a disordered wire in Appendix C. The matching of the correlators (14) and (15) to the leading order in g reflects the duality between interactions and quenched disorder discussed in this paper.

V. CONCLUSION

In summary, we have demonstrated the equivalence of a class of disorder-free interacting systems to noninteracting disordered systems. The interacting systems that allow for this mapping include dilute quantum gases of trapped ultracold particles and nodal semimetals, in which the screening of the interactions is suppressed due to the vanishing DoS near the node. The mapping may also be applied to interacting systems with large Fermi surfaces if the screening has no qualitative effect on the observable quantities, e.g., does not change the universality class of a phase transition.

Furthermore, the mapping allows us to predict new phenomena, e.g., phase transitions, in disordered and interacting systems dual to previously known phenomena. The duality can also be applied to map interacting systems to non-Hermitian disordered systems (by, e.g., applying the version of the mapping to attractive interactions to systems with repulsive interactions or by skipping the ‘‘Hermitization’’ step in the described construction of the mapping). It can thus be used to explore and describe phase transitions and other phenomena in systems described by non-Hermitian Hamiltonians [59–63], which we leave for future studies.

Using this mapping, we predict novel non-Anderson disorder-driven transitions, such as the disorder-driven transition in nodal semimetals dual to the BEC-vacuum transition known previously for interacting bosonic systems. We confirm the existence of such a transition by rigorous microscopic calculations. Based on the established duality we also expect a novel disorder-driven transition in 3D nodal-line semimetals and new interaction-driven transitions in systems with power-law dispersions.

Other questions that remain to be investigated are the role of the nonperturbative (instantonic) effects on the predicted phenomena as well as the possibility of spontaneously generated relevant operators that may change the criticality at the phase transitions [64].

ACKNOWLEDGMENTS

We are grateful to B. Sbierski, L. Radzihovsky, and S. Zhu for insightful discussions and comments on the paper. We have also benefited from discussion with Ya. Rodionov at the early stages of the project.

APPENDIX A: DETAILS OF THE MAPPING TO ALL ORDERS OF THE PERTURBATION THEORY

In this section, we provide detailed calculations of the equivalent diagrams in disordered noninteracting and

interacting disorder-free systems. As an example of an observable quantity in the interacting system, we use the density of particles, dual to the quantity ρ_s given by Eq. (5) in the disordered system. The density of particles and the quantity ρ_s are represented by sets of diagrams in Figs. 3(a) and 3(d). Basic elements of the diagrammatic technique are shown in Fig. 2. Here we do not assume a specific form of the interaction potential, and the disorder correlation in the dual system is determined by the form of the interaction potential. We describe first a generic diagram for an interacting system and demonstrate its equivalence to the corresponding diagram for the noninteracting disordered system. Then we provide explicit expressions for several lowest-order diagrams in both systems.

The value of each diagram with N interaction propagators contributing to the density of particles in the interacting system is given by

$$(-1)^{N+F} \frac{T^{N+1}}{V^{N+1}} \sum_{\omega, \mathbf{p}} \frac{1}{(i\omega_1 - \xi_{\mathbf{p}_1})^2} \frac{1}{i\omega_2 - \xi_{\mathbf{p}_2}} \dots \frac{1}{i\omega_{2N} - \xi_{\mathbf{p}_{2N}}} D(\Omega_1, \mathbf{P}_1) \dots D(\Omega_N, \mathbf{P}_N), \quad (A1)$$

where $F = 1$ for fermionic particles and $F = 0$ for bosonic particles, $D(\Omega_i, \mathbf{P}_i)$ is the interaction propagator which depends on the bosonic (fermionic) Matsubara frequency $\Omega_i = 2\pi T n_i$ [$\Omega_i = \pi T(2n_i + 1)$], and momentum \mathbf{P}_i and is the Fourier-transform of the interaction propagator

$$D(\mathbf{r}, \tau; \mathbf{r}', \tau') = -\langle T_\tau \hat{\phi}(\mathbf{r}, \tau) \hat{\phi}(\mathbf{r}', \tau') \rangle \quad (A2)$$

in the coordinate and Matsubara-time representation, where $\hat{\phi}$ are the bosonic fields corresponding to the interaction between the particles. The summation $\sum_{\omega, \mathbf{p}} \dots$ in Eq. (A1) may be carried out over any $N + 1$ independent frequencies and momenta, with the other frequency and momenta of the particle and interaction propagators determined from the energy and momentum conservation laws in the diagram. We assume the convergence of the sum for each diagram.

Because the bosonic propagator $D(\Omega_i, \mathbf{P}_i)$ is an even function of the Matsubara frequency Ω_i , each summation with respect to Matsubara frequencies ω in Eq. (A1) can be replaced with two summations with respect to ω and $-\omega$, $\sum_{\omega} \dots = \frac{1}{2} \sum_{\omega} \dots + \frac{1}{2} \sum_{-\omega} \dots$, which gives

$$(-1)^{N+F} \frac{T^{N+1}}{2V^{N+1}} \sum_{l=0,1} \sum_{\omega, \mathbf{p}} \frac{1}{[(-1)^l i\omega_1 - \xi_{\mathbf{p}_1}]^2} \frac{1}{(-1)^l i\omega_2 - \xi_{\mathbf{p}_2}} \dots \frac{1}{(-1)^l i\omega_{2N} - \xi_{\mathbf{p}_{2N}}} D(\Omega_1, \mathbf{P}_1) \dots D(\Omega_N, \mathbf{P}_N). \quad (A3)$$

Below we compare the expression (A3) for the N -th-order diagram for an interacting disorder-free system to the value of a similar diagram in the equivalent disordered noninteracting system.

In what immediately follows, we assume that the equivalent disordered system described by the Hamiltonian (2) has the volume $V \ell_{d+1}$ in the dimension $d + 1$, where ℓ_{d+1} is its length along one dimension and V is the cross section in the

remaining d dimensions. The topologically equivalent N th order diagram is given by

$$\frac{(-1)^{N+F}}{V^{N+1} \ell_{d+1}^{N+1}} \sum_{\mathbf{p}, k} \text{Tr} \left[\hat{\sigma}_z \frac{1}{-k_1 \hat{\sigma}_y - \xi_{\mathbf{p}_1} \hat{\sigma}_z} \frac{1}{2} \frac{1}{-k_1 \hat{\sigma}_y - \xi_{\mathbf{p}_1} \hat{\sigma}_z} \hat{\sigma}_z \dots \hat{\sigma}_z \frac{1}{-k_{2N} \hat{\sigma}_y - \xi_{\mathbf{p}_{2N}} \hat{\sigma}_z} \right] \tilde{D}(K_1, \mathbf{P}_1) \dots \tilde{D}(K_N, \mathbf{P}_N), \quad (\text{A4})$$

where (\mathbf{p}_i, k_i) is a $d+1$ -dimensional momentum; $i = 0, 1, \dots, 2N-1$; $\text{Tr} \dots$ is taken with respect to the pseudospin degrees of freedom; (anti-)periodic boundary conditions have to be chosen along the $d+1$ -st dimension for (fermionic) bosonic particles in the interacting system; and $-\tilde{D}(K_i, \mathbf{P}_i)$ is the ‘‘impurity line’’ [34], the Fourier-transform of the correlator

$$-\tilde{D}(\boldsymbol{\rho} - \boldsymbol{\rho}') = \langle u(\boldsymbol{\rho}) u(\boldsymbol{\rho}') \rangle_{\text{dis}} \quad (\text{A5})$$

of the random potential $u(\boldsymbol{\rho})$. Here, in accordance with the common convention, the impurity line (cf. Fig. 2) is defined to be positive for a real random potential. Similarly to the case of the diagram for the interacting system, the summation in Eq. (A4) may be carried out over any $N+1$ independent momenta in the dimension $d+1$, while the other momenta of the particle and disorder propagators are determined from the law of momentum conservation. In Eq. (A4), we took into account that the quantity ρ_s , to which the respective diagram contributes, corresponds to the $\hat{\sigma}_z/2$ vertex and to the particle propagator

$$\begin{aligned} (-k_i \hat{\sigma}_y - \xi_{\mathbf{p}_i} \hat{\sigma}_z)^{-1} &= \frac{1}{2} [G^A(k_i, \mathbf{p}_i, E=0) \\ &+ G^R(k_i, \mathbf{p}_i, E=0)], \end{aligned} \quad (\text{A6})$$

where G^A and G^R are the advanced and retarded Green’s functions of a free particle.

Equation (A4) gives

$$\frac{(-1)^{N+F}}{2V^{N+1} \ell_{d+1}^{N+1}} \sum_{\mathbf{p}, k} \text{Tr} \left[\frac{1}{ik_1 \hat{\sigma}_x - \xi_{\mathbf{p}_1} \mathbb{1}_{2 \times 2}} \frac{1}{ik_1 \hat{\sigma}_x - \xi_{\mathbf{p}_1} \mathbb{1}_{2 \times 2}} \dots \frac{1}{ik_{2N} \hat{\sigma}_x - \xi_{\mathbf{p}_{2N}} \mathbb{1}_{2 \times 2}} \right] \tilde{D}(K_1, \mathbf{P}_1) \dots \tilde{D}(K_N, \mathbf{P}_N), \quad (\text{A7})$$

where $\mathbb{1}_{2 \times 2}$ is the identity matrix in the pseudospin space. Because the eigenvalues of the operator $\hat{\sigma}_x$ are given by $(-1)^I$ with $I = 0, 1$, Eq. (A7) can be rewritten as

$$\frac{(-1)^{N+F}}{2V^{N+1} \ell_{d+1}^{N+1}} \sum_{I=0,1} \sum_{\mathbf{p}, k} \left[\frac{1}{i(-1)^I k_1 - \xi_{\mathbf{p}_1}} \frac{1}{i(-1)^I k_1 - \xi_{\mathbf{p}_1}} \dots \frac{1}{i(-1)^I k_{2N} - \xi_{\mathbf{p}_{2N}}} \right] \tilde{D}(K_1, \mathbf{P}_1) \dots \tilde{D}(K_N, \mathbf{P}_N). \quad (\text{A8})$$

Equations (A3) and (A8) for the diagrams for, respectively, the interacting disorder-free and noninteracting disordered systems are identical to each other so long as $\ell_{d+1} = 1/T$ and the Matsubara frequencies ω_i in Eq. (A3) match the values of the momenta k_i in Eq. (A8). The latter condition, with

$k_i = 2\pi T n_i$ ($k_i = 2\pi T n_i + \pi T$) and integer n_i , is satisfied if (anti-)periodic boundary conditions are imposed on the disordered system in the case of a (fermionic) bosonic interacting system.

In summary, we have established the correspondence, to all orders of the perturbation theory, between observables in a d -dimensional bosonic (fermionic) interacting disorder-free system at temperature T and a dual $d+1$ -dimensional noninteracting disordered system of length $\ell_{d+1} = 1/T$ with (anti-)periodic boundary conditions along the $d+1$ -st dimension. We focused on the observable quantities

$$\langle \hat{n}(\mathbf{r}) \rangle = \langle \hat{\rho}_s(\boldsymbol{\rho}) \rangle_{\text{dis}}, \quad (\text{A9})$$

where \hat{n} is the density of particles in the interacting system and the operator ρ_s in the disordered system is defined by Eq. (5). The established equivalence applies, however, to other observables, such as currents and spin/valley degrees of freedom and their correlators. To further illustrate the discussed duality, we consider below the zeroth and first order diagrams contributing to $\langle \hat{n}(\mathbf{r}) \rangle$ and $\langle \hat{\rho}_s(\boldsymbol{\rho}) \rangle_{\text{dis}}$ explicitly.

1. Zeroth order

The concentration of particles at the zeroth order is given by

$$\langle \hat{n}^{(0)}(\mathbf{r}) \rangle = \frac{T}{V} \sum'_{\omega, \mathbf{p}} \frac{(-1)^F}{i\omega - \xi_{\mathbf{p}}} = \frac{1}{V} \sum_{\mathbf{p}} \frac{1}{\exp(\xi_{\mathbf{p}}/T) \mp 1}, \quad (\text{A10})$$

where \sum' is our convention for the regularized sum over Matsubara frequencies (which amounts to, e.g., infinitesimal phase corrections to the frequencies [35] $i\omega \rightarrow i\omega e^{-i\omega\delta}$), ensuring that the sum of a Matsubara Green’s function over frequencies gives the Bose (Fermi) distribution function for bosonic (fermionic) frequencies.

For the disordered system, the zeroth-order contribution to the dual observable is given by

$$\begin{aligned} \langle \rho_s^{(0)}(\boldsymbol{\rho}) \rangle_{\text{dis}} &= \frac{(-1)^F}{V \ell_{d+1}} \sum'_{\mathbf{p}, k} \text{Tr} \left[\frac{\hat{\sigma}_z}{2} \frac{1}{-k \hat{\sigma}_y - \xi_{\mathbf{p}} \hat{\sigma}_z} \right] \\ &= \frac{(-1)^F}{V \ell_{d+1}} \sum'_{\mathbf{p}, k} \frac{-\xi_{\mathbf{p}}}{k^2 + \xi_{\mathbf{p}}^2} \\ &= \frac{1}{V} \sum'_{\mathbf{p}} \frac{1}{\exp(\xi_{\mathbf{p}} \ell_{d+1}) \pm 1}, \end{aligned} \quad (\text{A11})$$

where ‘‘+’’ and ‘‘-’’ correspond, respectively, to periodic and antiperiodic boundary conditions along the $d+1$ -st dimension, resulting in the quantized values $k = 2\pi \ell_{d+1}^{-1} n$ and $k = \pi \ell_{d+1}^{-1} (2n+1)$ of the momentum k . Equations (A10) and (A11) are precisely equivalent for $\ell_{d+1} = 1/T$, in accordance with the duality transformation derived in this paper.

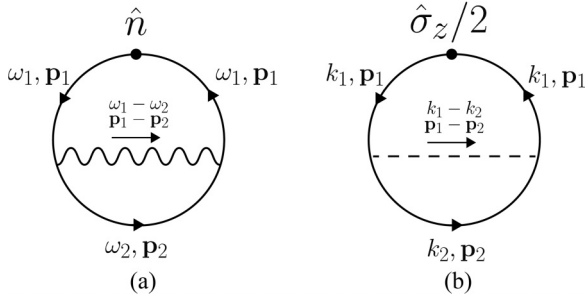


FIG. 5. First-order diagrams for the density \hat{n} in interacting disorder-free (a) and the operator ρ_s in noninteracting disordered (b) systems.

2. First order

Figure 5(a) shows the first-order correction to $\langle \hat{n} \rangle$. This diagram contributes

$$(-1)^{F+1} \frac{T^2}{V^2} \sum_{\omega_1, \omega_2, \mathbf{p}_1, \mathbf{p}_2} \frac{1}{(i\omega_1 - \xi_{\mathbf{p}_1})^2} \frac{1}{i\omega_2 - \xi_{\mathbf{p}_2}} \times D(\omega_1 - \omega_2, \mathbf{p}_1 - \mathbf{p}_2). \quad (\text{A12})$$

Again, because the bosonic propagator is even under the inversion of Matsubara frequency, $D(\omega_1 - \omega_2, \mathbf{p}_1 - \mathbf{p}_2) = D(-\omega_1 + \omega_2, \mathbf{p}_1 - \mathbf{p}_2)$, the sum with respect to the frequencies in Eq. (A12) is equivalent to two sums with respect to ω_1, ω_2 and $-\omega_1, -\omega_2$, $\sum_{\omega_1, \omega_2} \dots = \frac{1}{2} \sum_{\omega_1, \omega_2} \dots + \frac{1}{2} \sum_{-\omega_1, -\omega_2} \dots$. Therefore, Eq. (A12) becomes

$$(-1)^{F+1} \frac{T^2}{2V^2} \sum_{\omega_1, \omega_2, \mathbf{p}_1, \mathbf{p}_2} \left[\frac{1}{(i\omega_1 - \xi_{\mathbf{p}_1})^2} \frac{1}{i\omega_2 - \xi_{\mathbf{p}_2}} + \frac{1}{(-i\omega_1 - \xi_{\mathbf{p}_1})^2} \frac{1}{-i\omega_2 - \xi_{\mathbf{p}_2}} \right] D(\omega_1 - \omega_2, \mathbf{p}_1 - \mathbf{p}_2). \quad (\text{A13})$$

The corresponding diagram for the noninteracting disordered system is shown in Fig. 5(b) and is given by

$$\begin{aligned} & \frac{(-1)^F}{V^2 \ell_{d+1}^2} \sum_{\mathbf{p}_1, \mathbf{p}_2, k_1, k_2} \text{Tr} \left[\hat{\sigma}_z \frac{1}{-k_1 \hat{\sigma}_y - \xi_{\mathbf{p}_1} \hat{\sigma}_z} \frac{\hat{\sigma}_z}{2} \frac{1}{-k_1 \hat{\sigma}_y - \xi_{\mathbf{p}_1} \hat{\sigma}_z} \hat{\sigma}_z \frac{1}{-k_2 \hat{\sigma}_y - \xi_{\mathbf{p}_2} \hat{\sigma}_z} \right] [-\tilde{D}(k_1 - k_2, \mathbf{p}_1 - \mathbf{p}_2)] \\ &= \frac{(-1)^{F+1}}{2V^2 \ell_{d+1}^2} \sum_{\mathbf{p}_1, \mathbf{p}_2, k_1, k_2} \text{Tr} \left[\frac{1}{ik_1 \hat{\sigma}_x - \xi_{\mathbf{p}_1} \mathbb{1}_{2 \times 2}} \frac{1}{ik_1 \hat{\sigma}_x - \xi_{\mathbf{p}_1} \mathbb{1}_{2 \times 2}} \frac{1}{ik_2 \hat{\sigma}_x - \xi_{\mathbf{p}_2} \mathbb{1}_{2 \times 2}} \right] \tilde{D}(k_1 - k_2, \mathbf{p}_1 - \mathbf{p}_2). \end{aligned} \quad (\text{A14})$$

Taking the trace with respect to the eigenvalues of $\hat{\sigma}_x$ gives

$$\frac{(-1)^{F+1}}{2V^2 \ell_{d+1}^2} \sum_{\mathbf{p}_1, \mathbf{p}_2, k_1, k_2} \left(\frac{1}{ik_1 - \xi_{\mathbf{p}_1}} \frac{1}{ik_1 - \xi_{\mathbf{p}_1}} \frac{1}{ik_2 - \xi_{\mathbf{p}_2}} + \frac{1}{-ik_1 - \xi_{\mathbf{p}_1}} \frac{1}{-ik_1 - \xi_{\mathbf{p}_1}} \frac{1}{-ik_2 - \xi_{\mathbf{p}_2}} \right) \tilde{D}(k_1 - k_2, \mathbf{p}_1 - \mathbf{p}_2). \quad (\text{A15})$$

Since the values of ω_i and k_i match, due to the choice of the boundary conditions, and $\ell_{d+1} = 1/T$, Eqs. (A13) and (A15) are identical.

APPENDIX B: RENORMALIZATION-GROUP APPROACH TO INTERACTING GASES AND HIGH-DIMENSIONAL SEMIMETALS

In this section, we describe the renormalization of interactions in gases of particles with the power-law dispersion $\xi_{\mathbf{k}} \propto k^\alpha$ and the renormalization of disorder in the dual class of systems, i.e., semimetals with the dispersion $\xi_{\mathbf{k}} \hat{\sigma}_z + k_{d+1} \hat{\sigma}_y$. We demonstrate that these renormalizations are described by the same RG flow equation (11), which illustrates that these systems exhibit interaction-driven (disorder-driven) phase transitions in the same universality class.

The RG procedure for the interacting system involves repeatedly integrating out shells of largest momenta and frequencies,

$$Ke^{-l} \ll |\mathbf{k}| \ll K, \quad (\text{B1a})$$

$$|\xi_{Ke^{-l}}| \ll \omega \ll |\xi_K|, \quad (\text{B1b})$$

and renormalizing the properties of the systems perturbatively in the coupling constant g . The details of the cutoff procedure are not important in the one-loop approximation for the dimension d near the critical dimension $d_c = \alpha$. The diagrams

for the one-loop renormalization of the interaction propagator are shown in Figs. 6(a)–6(e). When evaluating them, it is sufficient to set all external incoming and outgoing frequencies and momenta to zero and sum/integrate only with respect to intermediate frequencies and momenta. The main contribution comes from Fig. 6(c):

$$[6c] = g^2 T \sum_{i\omega} \int_{\mathbf{k}} \frac{1}{i\omega - \xi_{\mathbf{k}}} \otimes \frac{1}{-i\omega - \xi_{-\mathbf{k}}}, \quad (\text{B2})$$

where the frequency summation and integration with respect to the momentum \mathbf{k} are carried out over the intervals (B1a)–(B1b); $\int_{\mathbf{k}} \dots = \int \frac{d^d \mathbf{k}}{(2\pi)^d} \dots$; the dispersion $\xi_{\mathbf{k}} \propto k^\alpha$ has the power dependence on the momentum \mathbf{k} but may also have additional structure in the valley or spin space; \otimes is the product of the spin/valley subspaces corresponding to the top and bottom propagators in Fig. 6(c).

We consider the case of large ultraviolet momentum cutoffs K and Ke^{-l} , corresponding to the kinetic energies significantly exceeding the temperature T . This allows us to replace the summation with respect to frequencies in Eq. (B2) by integration, $T \sum_{i\omega} \dots \rightarrow \int \frac{d\omega}{2\pi} \dots$. For a scalar dispersion

$$\xi_{\mathbf{k}} = |\mathbf{k}|^\alpha, \quad (\text{B3})$$

which has no valley and spin structure, the renormalized interaction propagator also has a trivial structure ($\propto \mathbb{1} \otimes \mathbb{1}$) in

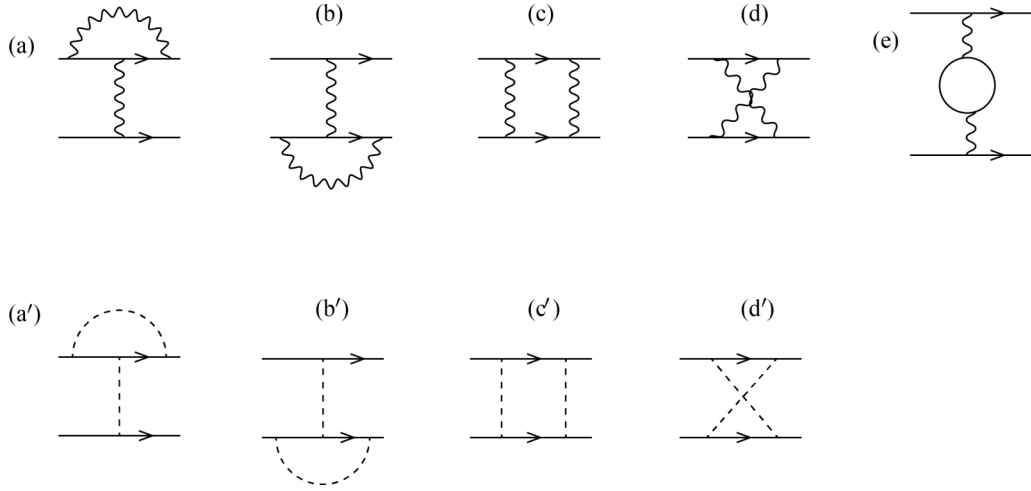


FIG. 6. Diagrams for the renormalization of the coupling constants in an interacting disorder-free [(a)–(e)] and noninteracting disordered [(a')–(d')] systems.

the spin/valley space, and the value of Fig. 6(c) is given by

$$[6c] = \frac{g^2 S_d K^{d-\alpha}}{2(2\pi)^d} \frac{1 - e^{-(d-\alpha)l}}{d - \alpha}. \quad (\text{B4})$$

All the other contributions shown in Fig. 6 may be estimated as

$$[6a] \sim [6b] \sim [6d] \sim [6e] \sim \frac{g^2 S_d K^{d-\alpha}}{2(2\pi)^d} \quad (\text{B5})$$

and are suppressed for the dimensions d close to the critical dimension $d_c = \alpha$. This leads to the RG flow equation for the coupling g given by

$$\partial_l g = \frac{S_d K^{d-\alpha}}{2(2\pi)^d} g^2. \quad (\text{B6})$$

Introducing the dimensionless coupling constant

$$\gamma = \frac{S_d}{2(2\pi)^d} g K^{d-\alpha} \quad (\text{B7})$$

gives the one-loop RG flow equation

$$\partial_l \gamma = (\alpha - d)\gamma + \gamma^2. \quad (\text{B8})$$

It is possible to show that the RG flow equation (B8) is exact, i.e., applies beyond the one-loop approximation. It has been noticed in Ref. [18] that the renormalized contact interaction between quadratically dispersive bosonic particles is given by the ladder diagrams shown in Fig. 7 and is, therefore, corresponding to the solution of the RG equation (B8). This result can be straightforwardly generalized to the case of the power-law dispersion $\xi_{\mathbf{k}} = k^\alpha$ considered here. The RG flow is terminated at the value of the ultraviolet cutoff K equal to the inverse size L^{-1} or a characteristic momentum scale corresponding to the renormalized kinetic energy on the order of the temperature T or the chemical potential μ .

The diagrams for the renormalization in the dual disordered noninteracting system, described by the Hamiltonian (2), are shown in Figs. 6(a')–6(d'). They are topologically equivalent to Figs. 6(a)–6(d) and do not include a diagram with a closed loop of particle propagators. In the diagrammatic technique for the disordered systems [34], contributions with loops are absent by construction. Although such loops are present for the interacting systems we consider, their contribution is suppressed due to the suppressed density of states at the chemical potential assumed in this paper.

The main contribution to the renormalization of the coupling g in the disordered system comes from Fig. 6(c'). While the other contributions to the renormalization are suppressed, it is convenient to evaluate together Figs. 6(c') and 6(d')

$$\begin{aligned} 6c' + 6d' &= g^2 \int_{\mathbf{p}} \int_{p_{d+1}} \hat{\sigma}_z \left(\frac{1}{\xi_{\mathbf{p}} \hat{\sigma}_z + p_{d+1} \hat{\sigma}_y} + \frac{1}{\xi_{-\mathbf{p}} \hat{\sigma}_z - p_{d+1} \hat{\sigma}_y} \right) \hat{\sigma}_z \otimes \hat{\sigma}_z \frac{1}{\xi_{\mathbf{p}} \hat{\sigma}_z + p_{d+1} \hat{\sigma}_y} \hat{\sigma}_z \\ &= g^2 \int_{\mathbf{p}} \int_{p_{d+1}} \frac{2\xi_{\mathbf{p}} \hat{\sigma}_z}{\xi_{\mathbf{p}}^2 + p_{d+1}^2} \otimes \frac{\hat{\sigma}_z (\xi_{\mathbf{p}} \hat{\sigma}_z + p_{d+1} \hat{\sigma}_y) \hat{\sigma}_z}{\xi_{\mathbf{p}}^2 + p_{d+1}^2} = g^2 \int_{\mathbf{p}} \int_{p_{d+1}} \frac{2\xi_{\mathbf{p}}^2}{[\xi_{\mathbf{p}}^2 + p_{d+1}^2]^2} \hat{\sigma}_z \otimes \hat{\sigma}_z \approx \frac{g^2 S_d K^{d-\alpha}}{2(2\pi)^d} \frac{1 - e^{-(d-\alpha)l}}{d - \alpha}. \end{aligned} \quad (\text{B9})$$

Similarly to the case of interacting systems, it is possible to demonstrate that the contributions of the other diagrams to the renormalization of the coupling g are suppressed, and the

flow of the coupling is again described by Eq. (B8). Identical RG flows for the coupling in the cases of interacting disorder-free and noninteracting disordered systems illustrate the

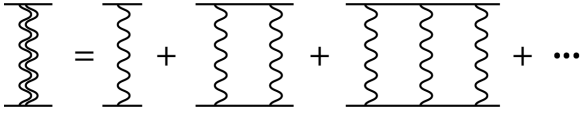


FIG. 7. Ladder diagrams for the renormalization of the interaction between bosonic particles in vacuum.

equivalence between the two classes of systems discussed in this paper.

Both of these classes of systems display transitions at the critical value of the dimensionless coupling $\gamma_c = d - \alpha$ between the phases with irrelevant interactions (disorder), for subcritical coupling, and relevant interactions (disorder), for supercritical interactions (disorder). For the example of the disordered-driven transition considered here, the universality classes of the dual transitions match exactly, owing to the absence of screening of the interactions in the vacuum phase of the interacting system at zero temperature and chemical potential. If the interacting system has a small chemical potential μ or temperature T , then the mapping becomes approximate. At small values of $K_{\text{ir}} = [\min(|\mu|, T)]^{\frac{1}{d}} \ll K_0$, however, the mapping will still be accurate, as is clear from comparing the value of the loop diagram [6e] $\sim g^2 \frac{S_d}{(2\alpha\pi)^d} K_{\text{ir}}^{d-\alpha}$ to the contribution of the diagram [6c].

We emphasize that the phenomenology of the novel disorder-driven transition predicted here is similar to the

phenomenology of the non-Anderson disorder-driven transitions [7] studied previously for systems with isotropic dispersions $\xi_{\mathbf{k}} \propto k^\delta$ in dimensions $\tilde{d} > 2\delta$: renormalized disorder in such systems vanishes for subcritical values of the disorder strength and is finite otherwise. The RG equations for the flow of the dimensionless disorder strength for such systems are given by

$$\partial_\ell \gamma = (2\delta - \tilde{d})\gamma + \gamma^2 + \mathcal{O}(\gamma^3) \quad (\text{B10})$$

and in one loop are also given by the diagrams shown in Figs. 6(a')–6(d'). We emphasize that for generic symmetries of quenched disorder all of these four diagrams may give contributions of the same order of magnitude to the renormalization and the higher-loop contributions and in general are non-negligible (see, e.g., Ref. [50]).

The disorder-driven transitions considered in this paper, equivalent to the interaction-driven BEC-vacuum transitions in interacting systems, are an extension of the previously studied non-Anderson disorder-driven transitions to the case of systems with an anisotropic dispersion $\propto \hat{\sigma}_z \xi_{\mathbf{p}} + \hat{\sigma}_y p_{d+1}$, which is linear along one direction and has a power-law form $\xi_{\mathbf{p}} \propto p^\alpha$ along the other d dimensions. The lower-critical dimension for the non-Anderson disorder-driven transitions in such systems is given by $\tilde{d} \equiv d + 1 = \alpha + 1$. The vanishing of the high-order contributions in the RG flow (B8) is a consequence of the disorder symmetry ($\propto u\hat{\sigma}_z$) in such systems.

APPENDIX C: DETAILS OF THE DUALITY BETWEEN QUANTUM DOT AND 1D WIRES

In this section, we provide the details of the duality mapping between the one-site Hubbard model (quantum dot) described by the Hamiltonian (12) and a disordered 1D wire described by the Hamiltonian (13). The Hamiltonian of the quantum dot can be rewritten in the equivalent form

$$\hat{\mathcal{H}}_{\text{dot}} = \xi \hat{n}_\uparrow + \xi \hat{n}_\downarrow - g \hat{n}_\uparrow \hat{n}_\downarrow = \left(\xi + \frac{g}{2}\right) \hat{n}_\uparrow + \left(\xi + \frac{g}{2}\right) \hat{n}_\downarrow - \frac{g}{2} (\hat{n}_\uparrow + \hat{n}_\downarrow)^2, \quad (\text{C1})$$

where we have used that $\hat{n}_{\uparrow,\downarrow}^2 \equiv \hat{n}_{\uparrow,\downarrow}$. Observables in a system described by the Hamiltonian (C1) can be represented in the form of a path integral over Grassmann variables

$$\langle \dots \rangle = \int \mathcal{D}\bar{\Psi} \mathcal{D}\Psi \dots \exp \left\{ - \int_0^\beta \sum_{i=\uparrow,\downarrow} \bar{\Psi}_i(\tau) \left[\partial_\tau + \xi + \frac{g}{2} \right] \Psi_i(\tau) d\tau - \frac{g}{2} \int_0^\beta \left[\sum_{i=\uparrow,\downarrow} \bar{\Psi}_i(\tau) \Psi_i(\tau) \right]^2 d\tau \right\}, \quad (\text{C2})$$

where the preexponential \dots corresponds to the operator of the observable expressed in terms of the Grassmann fields $\bar{\Psi}$ and Ψ . Decoupling the quartic term by a bosonic field ϕ gives

$$\langle \dots \rangle = \int \mathcal{D}\bar{\Psi} \mathcal{D}\Psi \mathcal{D}\phi \dots \exp \left\{ - \int_0^\beta \sum_{i=\uparrow,\downarrow} \bar{\Psi}_i(\tau) \left[\partial_\tau + \xi + \frac{g}{2} + \phi(\tau) \right] \Psi_i(\tau) d\tau - \frac{1}{2g} \int_0^\beta \phi^2(\tau) d\tau \right\}. \quad (\text{C3})$$

The action describing the observable in Eq. (C3) corresponds to spin-1/2 fermions interacting with bosons whose propagator is given by $\langle \phi(\tau) \phi(\tau') \rangle = g\delta(\tau - \tau')$.

Applying the duality transformation developed in this paper, this model may be mapped to a 1D model with quenched disorder, with the Matsubara time τ mapped to the coordinate x of the 1D model and with the bosonic field $\phi(\tau)$ mapped to a random potential $u(x)$. The Hamiltonian of this 1D model is given by

$$\hat{\mathcal{H}}_{\text{wire}} = \sum_{i=\uparrow,\downarrow} \hat{\Psi}_i(x) [\xi \hat{\sigma}_z - i \hat{\sigma}_y \partial_x + u(x) \hat{\sigma}_z] \hat{\Psi}_i(x). \quad (\text{C4})$$

We emphasize that, strictly speaking, the quantum dot described by the Hamiltonian (C1) does not satisfy the assumptions about the negligibility of screening and Hartree-type contributions, which correspond to diagrams with additional fermionic loops and are neglected in this paper when deriving the equivalence between interacting disorder-free and noninteracting

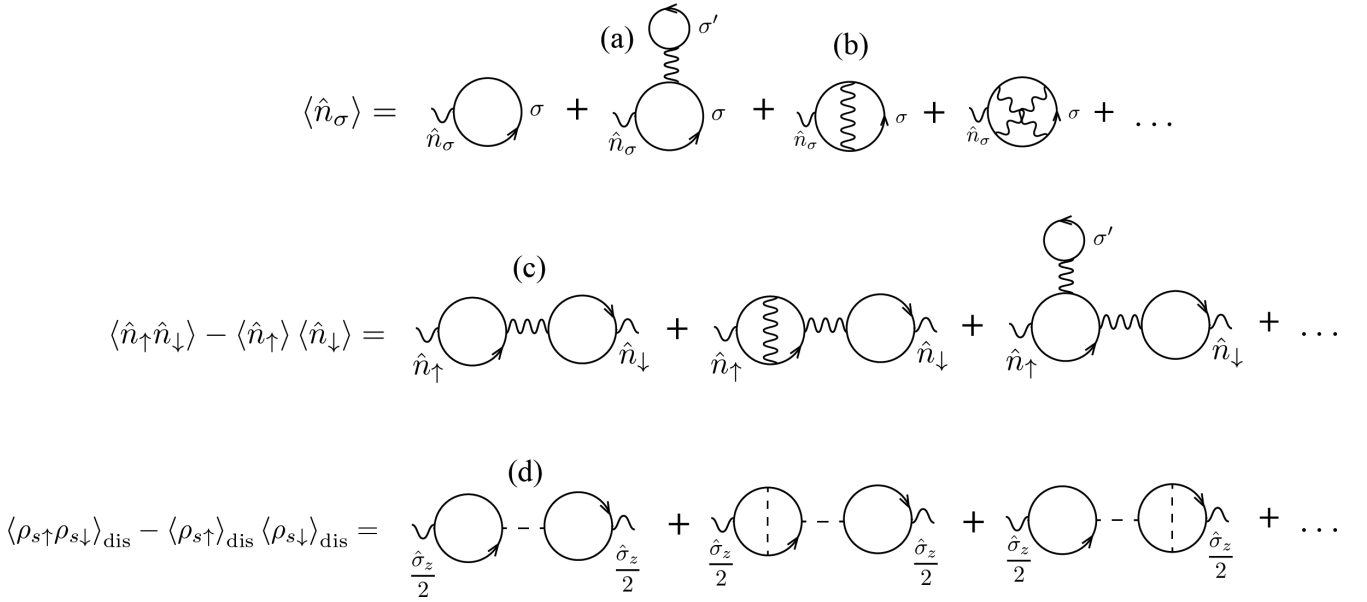


FIG. 8. Diagrams that contribute to the correlators K and K_{dis} in the one-site Hubbard model and a disordered wire described by the Hamiltonians (C1) and (C4).

disordered systems. For example, in Fig. 8(a) describes the Hartree contribution to the average occupation number $\langle \hat{n}_\sigma \rangle$ for the electron state with spin σ and is equal to Fig. 8(b), which we take into account when demonstrating the equivalence, and is, therefore, non-negligible.

However, observables in the quantum dot may still be mapped to observables in the disordered wire so long as they are unaffected by the screening and Hartree contributions. To illustrate this, we consider the leading contribution to the correlator

$$K = \langle \hat{n}_\uparrow \hat{n}_\downarrow \rangle - \langle \hat{n}_\uparrow \rangle \langle \hat{n}_\downarrow \rangle \quad (\text{C5})$$

of the occupation numbers with different spins in the quantum dot. In the equilibrium state at temperature T , the correlator is given by

$$K = \frac{\sum_{n_{\uparrow,\downarrow}=0,1} n_\uparrow n_\downarrow e^{-\frac{n_\uparrow \xi + n_\downarrow \xi - g n_\uparrow n_\downarrow}{T}}}{\sum_{n_{\uparrow,\downarrow}=0,1} e^{-\frac{n_\uparrow \xi + n_\downarrow \xi - g n_\uparrow n_\downarrow}{T}}} - \left(\frac{\sum_{n_{\uparrow,\downarrow}=0,1} n_\uparrow e^{-\frac{n_\uparrow \xi + n_\downarrow \xi - g n_\uparrow n_\downarrow}{T}}}{\sum_{n_{\uparrow,\downarrow}=0,1} e^{-\frac{n_\uparrow \xi + n_\downarrow \xi - g n_\uparrow n_\downarrow}{T}}} \right)^2 \quad (\text{C6})$$

$$\approx \frac{g}{T} \left[\frac{e^{\xi/T}}{(1 + e^{\xi/T})^2} \right]^2, \quad (\text{C7})$$

where we kept only the leading in g contribution. The correlator (C5) can also be found diagrammatically, as shown in Fig. 8. The leading in the coupling g contribution is given by

$$K = [8c] + o(g^2) = \frac{g}{T} \left[\frac{e^{\xi/T}}{(1 + e^{\xi/T})^2} \right]^2 + o(g^2). \quad (\text{C8})$$

Because this contribution does not contain fermionic loops mimicking the screening of the interactions or Hartree contributions, it allows for mapping to a similar correlator

$$K_{\text{dis}} = \langle \rho_{s\uparrow} \rho_{s\downarrow} \rangle_{\text{dis}} - \langle \rho_{s\uparrow} \rangle_{\text{dis}} \langle \rho_{s\downarrow} \rangle_{\text{dis}}. \quad (\text{C9})$$

in a disordered wire described by the Hamiltonian (C4). The diagrams for the correlator in the disordered system are shown in Fig. 8, where the leading-order contribution is equal to

$$\begin{aligned} K_{\text{dis}} &= [8d] + o(g^2) = \frac{g}{\ell_{d+1}^3} \sum_{k_1, k_2} \text{Tr} \left[\hat{\sigma}_z \frac{1}{-k_1 \hat{\sigma}_y - \xi \hat{\sigma}_z} \frac{\hat{\sigma}_z}{2} \frac{1}{-k_1 \hat{\sigma}_y - \xi \hat{\sigma}_z} \right] \text{Tr} \left[\hat{\sigma}_z \frac{1}{-k_2 \hat{\sigma}_y - \xi \hat{\sigma}_z} \frac{\hat{\sigma}_z}{2} \frac{1}{-k_2 \hat{\sigma}_y - \xi \hat{\sigma}_z} \right] + o(g^2) \\ &= \frac{g}{\ell_{d+1}^3} \sum_{k_1, k_2} \frac{-k_1^2 + \xi^2}{(k_1^2 + \xi^2)^2} \frac{-k_2^2 + \xi^2}{(k_2^2 + \xi^2)^2} = g \ell_{d+1} \left[\frac{e^{\xi \ell_{d+1}}}{(1 + e^{\xi \ell_{d+1}})^2} \right]^2 + o(g^2). \end{aligned} \quad (\text{C10})$$

Because the quantum dot described by the Hamiltonian (C1) is fermionic, the dual disordered wire described by the Hamiltonian (C4) has antiperiodic boundary conditions. At $\ell_{d+1} = 1/T$, Eqs. (C8) and (C10) for observables in, respectively, the quantum dot and the disordered wire are equivalent, which illustrates again the interactions-disorder duality shown in this paper.

-
- [1] R. Blankenbecler, D. J. Scalapino, and R. L. Sugar, Monte Carlo calculations of coupled boson-fermion systems. I, *Phys. Rev. D* **24**, 2278 (1981).
- [2] J. E. Hirsch, Discrete Hubbard-Stratonovich transformation for fermion lattice models, *Phys. Rev. B* **28**, 4059 (1983).
- [3] S. R. White, D. J. Scalapino, R. L. Sugar, N. E. Bickers, and R. T. Scalettar, Attractive and repulsive pairing interaction vertices for the two-dimensional Hubbard model, *Phys. Rev. B* **39**, 839 (1989).
- [4] K. B. Efetov, *Supersymmetry in Disorder and Chaos* (Cambridge University Press, New York, 1999).
- [5] A. Kamenev, *Field Theory of Non-Equilibrium Systems* (Cambridge University Press, Cambridge, UK, 2011).
- [6] D. Belitz and T. R. Kirkpatrick, The Anderson-Mott transition, *Rev. Mod. Phys.* **66**, 261 (1994).
- [7] S. V. Syzranov and L. Radzihovsky, High-dimensional disorder-driven phenomena in Weyl semimetals, semiconductors, and related systems, *Annu. Rev. Condens. Mater. Phys.* **9**, 35 (2018).
- [8] S. Zhu and S. Syzranov, BCS-like disorder-driven instabilities and ultraviolet effects in nodal-line semimetals *Annu. Phys.* **459**, 169501 (2023).
- [9] I. L. Aleiner and K. B. Efetov, Effect of disorder on transport in graphene, *Phys. Rev. Lett.* **97**, 236801 (2006).
- [10] V. Kozii, A. Klein, R. M. Fernandes, and J. Ruhman, Synergistic ferroelectricity and superconductivity in zero-density dirac semimetals near quantum criticality, *Phys. Rev. Lett.* **129**, 237001 (2022).
- [11] J. Maciejko and R. Nandkishore, Weyl semimetals with short-range interactions, *Phys. Rev. B* **90**, 035126 (2014).
- [12] E. Fradkin, Critical behavior of disordered degenerate semiconductors. I. Models, symmetries, and formalism, *Phys. Rev. B* **33**, 3257 (1986).
- [13] E. Fradkin, Critical behavior of disordered degenerate semiconductors. II. Spectrum and transport properties in mean-field theory, *Phys. Rev. B* **33**, 3263 (1986).
- [14] A. Rodríguez, V. A. Malyshev, G. Sierra, M. A. Martín-Delgado, J. Rodríguez-Laguna, and F. Domínguez-Adame, Anderson transition in low-dimensional disordered systems driven by long-range nonrandom hopping, *Phys. Rev. Lett.* **90**, 027404 (2003).
- [15] A. V. Malyshev, V. A. Malyshev, and F. Domínguez-Adame, Monitoring the localization-delocalization transition within a one-dimensional model with nonrandom long-range interaction, *Phys. Rev. B* **70**, 172202 (2004).
- [16] S. V. Syzranov, L. Radzihovsky, and V. Gurarie, Critical transport in weakly disordered semiconductors and semimetals, *Phys. Rev. Lett.* **114**, 166601 (2015).
- [17] S. V. Syzranov, V. Gurarie, and L. Radzihovsky, Unconventional localisation transition in high dimensions, *Phys. Rev. B* **91**, 035133 (2015).
- [18] D. Uzunov, On the zero temperature critical behaviour of the nonideal Bose gas, *Phys. Lett. A* **87**, 11 (1981).
- [19] P. Nikolic and S. Sachdev, Renormalization-group fixed points, universal phase diagram, and $1/N$ expansion for quantum liquids with interactions near the unitarity limit, *Phys. Rev. A* **75**, 033608 (2007).
- [20] V. Gurarie and L. Radzihovsky, Resonantly paired fermionic superfluids, *Ann. Phys.* **322**, 2 (2007).
- [21] P. Richerme, Z.-X. Gong, A. Lee, C. Senko, J. Smith, M. Foss-Feig, S. Michalakis, A. V. Gorshkov, and C. Monroe, Non-local propagation of correlations in quantum systems with long-range interactions, *Nature (London)* **511**, 198 (2014).
- [22] R. Islam, C. Senko, W. C. Campbell, S. Korenblit, J. Smith, A. Lee, E. E. Edwards, C.-C. J. Wang, J. K. Freericks, and C. Monroe, Emergence and frustration of magnetism with variable-range interactions in a quantum simulator, *Science* **340**, 583 (2013).
- [23] P. Jurcevic, B. P. Lanyon, P. Hauke, C. Hempel, P. Zoller, R. Blatt, and C. F. Roos, Quasiparticle engineering and entanglement propagation in a quantum many-body system, *Nature (London)* **511**, 202 (2014).
- [24] P. Jurcevic, P. Hauke, C. Maier, C. Hempel, B. P. Lanyon, R. Blatt, and C. F. Roos, Spectroscopy of interacting quasiparticles in trapped ions, *Phys. Rev. Lett.* **115**, 100501 (2015).
- [25] K. S. Tikhonov and M. V. Feigel'man, Strange metal state near quantum superconductor-metal transition in thin films, *Ann. Phys.* **417**, 168138 (2020).
- [26] S. V. Syzranov and V. Gurarie, Duality between disordered nodal semimetals and systems with power-law hopping, *Phys. Rev. Res.* **1**, 032035(R) (2019).
- [27] S. Sun and S. Syzranov, High-temperature criticality in systems with power-law interactions (unpublished).
- [28] K. B. Efetov, Quantum disordered systems with a direction, *Phys. Rev. B* **56**, 9630 (1997).
- [29] X. Luo, Z. Xiao, K. Kawabata, T. Ohtsuki, and R. Shindou, Unifying the anderson transitions in Hermitian and non-Hermitian systems, *Phys. Rev. Res.* **4**, L022035 (2022).
- [30] J. Feinberg and A. Zee, Non-Hermitian random matrix theory: Method of Hermitian reduction, *Nucl. Phys. B* **504**, 579 (1997).
- [31] Z. Gong, Y. Ashida, K. Kawabata, K. Takasan, S. Higashikawa, and M. Ueda, Topological phases of non-Hermitian systems, *Phys. Rev. X* **8**, 031079 (2018).
- [32] K. Kawabata, K. Shiozaki, M. Ueda, and M. Sato, Symmetry and topology in non-Hermitian physics, *Phys. Rev. X* **9**, 041015 (2019).
- [33] E. J. Bergholtz, J. C. Budich, and F. K. Kunst, Exceptional topology of non-Hermitian systems, *Rev. Mod. Phys.* **93**, 015005 (2021).
- [34] A. A. Abrikosov, L. P. Gorkov, and I. E. Dzyaloshinski, *Methods of Quantum Field Theory in Statistical Physics* (Dover, New York, 1975).

- [35] A. Altland and B. Simons, *Condensed Matter Field Theory* (Cambridge University Press, Cambridge, UK, 2006).
- [36] N. P. Armitage, E. J. Mele, and A. Vishwanath, Weyl and Dirac semimetals in three-dimensional solids, *Rev. Mod. Phys.* **90**, 015001 (2018).
- [37] T. Meng and L. Balents, Weyl superconductors, *Phys. Rev. B* **86**, 054504 (2012).
- [38] H. Wei, S.-P. Chao, and V. Aji, Excitonic phases from Weyl semimetals, *Phys. Rev. Lett.* **109**, 196403 (2012).
- [39] H. Wei, S.-P. Chao, and V. Aji, Odd-parity superconductivity in Weyl semimetals, *Phys. Rev. B* **89**, 014506 (2014).
- [40] G. Y. Cho, J. H. Bardarson, Y.-M. Lu, and J. E. Moore, Superconductivity of doped Weyl semimetals: Finite-momentum pairing and electronic analog of the $^3\text{He}-A$ phase, *Phys. Rev. B* **86**, 214514 (2012).
- [41] M. Trescher, E. J. Bergholtz, M. Udagawa, and J. Knolle, Charge density wave instabilities of type-II Weyl semimetals in a strong magnetic field, *Phys. Rev. B* **96**, 201101(R) (2017).
- [42] W. Shi, B. J. Wieder, H. L. Meyerheim, Y. Sun, Y. Zhang, Y. Li, L. Shen, Y. Qi, L. Yang, J. Jena, P. Werner, K. Koepf, S. Parkin, Y. Chen, C. Felser, B. A. Bernevig, and Z. Wang, A charge-density-wave topological semimetal, *Nat. Phys.* **17**, 381 (2021).
- [43] Exponentially rare non-perturbative effects (rare-region effects) may convert such transitions to sharp crossovers, as discussed recently in the context of 3D Weyl semimetals [17,51,65–69]. However, dual interacting transitions are true phase transitions as the described interactions-disorder duality applies only at the perturbative level and does not extend to rare-region effects.
- [44] R. Shindou and S. Murakami, Effects of disorder in three-dimensional Z_2 quantum spin Hall systems, *Phys. Rev. B* **79**, 045321 (2009).
- [45] P. Goswami and S. Chakravarty, Quantum criticality between topological and band insulators in $3 + 1$ dimensions, *Phys. Rev. Lett.* **107**, 196803 (2011).
- [46] S. Ryu and K. Nomura, Disorder-induced quantum phase transitions in three-dimensional topological insulators and superconductors, *Phys. Rev. B* **85**, 155138 (2012).
- [47] K. Kobayashi, T. Ohtsuki, K.-I. Imura, and I. F. Herbut, Density of states scaling at the semimetal to metal transition in three dimensional topological insulators, *Phys. Rev. Lett.* **112**, 016402 (2014).
- [48] T. Louvet, D. Carpentier, and A. A. Fedorenko, On the disorder-driven quantum transition in three-dimensional relativistic metals, *Phys. Rev. B* **94**, 220201(R) (2016).
- [49] B. Roy, R.-J. Slager, and V. Juričić, Global phase diagram of a dirty Weyl liquid and emergent superuniversality, *Phys. Rev. X* **8**, 031076 (2018).
- [50] S. V. Syzranov, P. M. Ostrovsky, V. Gurarie, and L. Radzihovsky, Critical exponents at the unconventional disorder-driven transition in a Weyl semimetal, *Phys. Rev. B* **93**, 155113 (2016).
- [51] J. H. Pixley, D. A. Huse, and S. Das Sarma, Rare-region-induced avoided quantum criticality in disordered three-dimensional Dirac and Weyl semimetals, *Phys. Rev. X* **6**, 021042 (2016).
- [52] B. Sbierski, E. J. Bergholtz, and P. W. Brouwer, Quantum critical exponents for a disordered three-dimensional Weyl node, *Phys. Rev. B* **92**, 115145 (2015).
- [53] S. Bera, J. D. Sau, and B. Roy, Dirty Weyl semimetals: Stability, phase transition, and quantum criticality, *Phys. Rev. B* **93**, 201302(R) (2016).
- [54] B. Sbierski, K. S. C. Decker, and P. W. Brouwer, Weyl node with random vector potential, *Phys. Rev. B* **94**, 220202(R) (2016).
- [55] S. Liu, T. Ohtsuki, and R. Shindou, Effect of disorder in three dimensional layered Chern insulator, *Phys. Rev. Lett.* **116**, 066401 (2016).
- [56] I. Balog, D. Carpentier, and A. A. Fedorenko, Disorder-driven quantum transition in relativistic semimetals: Functional renormalization via the porous medium equation, *Phys. Rev. Lett.* **121**, 166402 (2018).
- [57] X. Luo, B. Xu, T. Ohtsuki, and R. Shindou, Quantum multicriticality in disordered Weyl semimetals, *Phys. Rev. B* **97**, 045129 (2018).
- [58] M. Y. Veillette, D. E. Sheehy, and L. Radzihovsky, Large- N expansion for unitary superfluid Fermi gases, *Phys. Rev. A* **75**, 043614 (2007).
- [59] V. V. Konotop, J. Yang, and D. A. Zezyulin, Nonlinear waves in \mathcal{PT} -symmetric systems, *Rev. Mod. Phys.* **88**, 035002 (2016).
- [60] T. Yoshida, R. Peters, N. Kawakami, and Y. Hatsugai, Exceptional band touching for strongly correlated systems in equilibrium, *Prog. Theor. Exp. Phys.* **2020**, 12A109 (2020).
- [61] H. Varguet, B. Rousseaux, D. Dzsotjan, H. R. Jauslin, S. Guérin, and G. C. des Francs, Non-Hermitian Hamiltonian description for quantum plasmonics: from dissipative dressed atom picture to Fano states, *J. Phys. B: At., Mol. Opt. Phys.* **52**, 055404 (2019).
- [62] H. Shen, B. Zhen, and L. Fu, Topological band theory for non-Hermitian Hamiltonians, *Phys. Rev. Lett.* **120**, 146402 (2018).
- [63] N. Hatano and D. R. Nelson, Vortex pinning and non-Hermitian quantum mechanics, *Phys. Rev. B* **56**, 8651 (1997).
- [64] B. Sbierski and S. Syzranov, Non-Anderson critical scaling of the Thouless conductance in 1D, *Ann. Phys.* **418**, 168169 (2020).
- [65] F. Wegner, Bounds on the density of states in disordered systems, *Z. Phys. B* **44**, 9 (1981).
- [66] I. M. Suslov, Density of states near an Anderson transition in four-dimensional space: Lattice mode, *Sov. Phys. JETP* **79**, 307 (1994).
- [67] R. Nandkishore, D. A. Huse, and S. L. Sondhi, Rare region effects dominate weakly disordered 3D Dirac points, *Phys. Rev. B* **89**, 245110 (2014).
- [68] J. H. Wilson, D. A. Huse, S. Das Sarma, and J. H. Pixley, Avoided quantum criticality in exact numerical simulations of a single disordered Weyl cone, *Phys. Rev. B* **102**, 100201(R) (2020).
- [69] J. H. Pixley and J. H. Wilson, Rare regions and avoided quantum criticality in disordered Weyl semimetals and superconductors, *Ann. Phys.* **435**, 168455 (2021).